RSC Advances

PAPER

View Article Online
View Journal | View Issue

Cite this: *RSC Adv.*, 2022, **12**, 18296

Target-induced activation of DNAzyme for highly sensitive colorimetric detection of bleomycin *via* DNA scission†

Xiaofei Liao,[a] Mengyan Li[a] and Li Zou *[ab]

Received 4th May 2022
Accepted 16th June 2022

DOI: 10.1039/d2ra02816f

rsc.li/rsc-advances

In this work, a label-free and sensitive colorimetric sensing strategy for the detection of bleomycin (BLM) was developed on the basis of BLM-mediated activation of G-quadruplex DNAzyme *via* DNA strand scission. A G-quadruplex based hairpin probe (G4HP) containing the scission site (5′-GT-3′) of BLM at the loop region and guanine (G)-rich sequences at its 5′-end was employed in this protocol. In the presence of BLM, it may cleave the 5′-GT-3′ site of the hairpin probe with Fe(II) as a cofactor, releasing the G-tetrads DNA fragment, which may further bind hemin to form a catalytic G-quadruplex-hemin DNAzyme. The resultant G-quadruplex DNAzyme has notable peroxidase-like activity, which effectively catalyzes the oxidation of 2,2′-azino-bis(3-ethylbenzothiozoline-6-sulfonic acid) (ABTS) by H_2O_2 to produce the blue-green-colored free-radical cation ($ABTS^{\cdot+}$). Therefore, the detection of BLM can be achieved by observing the color transition with the naked eye or measuring the absorbance at a wavelength of 420 nm using a UV-Vis spectrophotometer. Attributing to the specific BLM-induced DNA strand scission and the effective locking of G-tetrads in the stem of the G4HP, the colorimetric sensing strategy exhibits high sensitivity and selectivity for detection of BLM in human serum samples, which might hold great promise for BLM assay in biomedical and clinical research.

Introduction

As a class of glycopeptide-derived antibiotics isolated from *Streptomyces* species, bleomycins (BLMs) have been widely used clinically in combination with chemotherapy for the treatment of various tumorous diseases due to their distinct advantages of low myelosuppression and low immunosuppression.[1–4] The antitumor activity of BLMs is generally attributed to the selective cleavage of single-stranded or double-stranded DNAs and possibly RNAs in the presence of oxygen and metal ions as cofactors.[5–7] However, an unsuitable dose of BLMs in clinical treatment also exhibits some serious dose-limiting side effects, such as renal and lung toxicity, and bad pulmonary fibrosis.[8,9] In order to achieve the desired therapeutic effect with a lower dose and toxicity, there is great anxiety to develop a reliable and sensitive method for the determination of trace amounts of BLM in both pharmaceutical analysis and clinical samples. Up to date, various methods for BLM detection have been developed, such as high-performance liquid chromatography (HPLC),[10] radioimmunoassay (RIA),[11] enzyme immunoassay (EIA),[12] microbiological assay,[13] colorimetric assay,[14] fluorescent assay[15–17] and electrochemical assay.[18,19] Among them, colorimetric methods have attracted significant attention due to the remarkable features of low cost, convenient operation, instrument simplicity and fast response.[20]

Recently, some colorimetric strategies have been reported for BLM assay based on the aggregation of gold nanoparticles (AuNPs),[14,21] but these methods suffer from poor specificity. An alternative approach has been developed for colorimetric detection of BLM based on BLM–Fe(II) complex catalyzed oxidation of 2,2′-azino-bis(3-ethylbenzothiozoline-6-sulfonic acid) (ABTS).[22] However, Fe(II)-based Fenton reaction is optimal at low pH,[23] which limits its scope of application. As reported, the BLM–Fe(II) complex can active molecular oxygen to generate a ternary complex BLM–Fe(III)OOH, which is able to selectively degrade DNA at a recognition site.[24,25] Various sensing strategies have been developed for the sensitive determination of BLM based on BLM–Fe(II) induced DNA strand scission.[26–29] For example, Ma *et al.* applied the specific scission of BLM to release G-tracts DNA fragment locked in the molecular beacon (MB), which self-assembles into a G-triplex-thioflavin T (ThT) complex with strong fluorescence emission.[30] He *et al.* reported a sensitive electrochemical assay for BLM detection based on BLM-mediated activation of Zn^{2+}-dependent DNAzyme and a MOF-modified electrode.[18] To the best of our knowledge, the application of BLM-induced DNA scission for colorimetric assay of BLM has not been reported

[a]*School of Pharmacy, Guangdong Pharmaceutical University, Guangzhou 510006, PR China. E-mail: lizou@gdpu.edu.cn*

[b]*Key Specialty of Clinical Pharmacy, The First Affiliated Hospital of Guangdong Pharmaceutical University, Guangzhou 510699, PR China*

† Electronic supplementary information (ESI) available. See https://doi.org/10.1039/d2ra02816f

yet. Therefore, it is still highly desirable to develop sensitive and label-free colorimetric sensing strategies for BLM detection.

Over the past decades, G-quadruplex DNAzyme has been widely applied in colorimetric, chemiluminescent and electrochemical assays because of its good stability, low cost and ease of synthesis.[31–36] More importantly, the peroxidase-like activity of G-quadruplex DNAzyme can be applied to efficiently catalyze the H_2O_2-mediated oxidation of ABTS to free-radical cation ($ABTS^{\cdot+}$) with an obvious color change from colorless to green. Furthermore, G-quadruplex DNAzyme can be designed ingeniously, such as G-quadruplex based label-free molecular beacon, to improve the selectivity and enhance the signal response. Inspired by the BLM–Fe(II) mediated DNA scission and the catalytic activity of G-quadruplex DNAzyme, we herein propose a label-free and sensitive colorimetric method for determination of BLM based on BLM-mediated activation of G-quadruplex DNAzyme *via* DNA strand scission. We design a G-quadruplex based hairpin probe (G4HP) containing the scission site (5′-GT-3′) of BLM at the loop region and guanine (G)-rich sequences at its 5′-end. The G4HP undergoes an irreversible cleavage event by BLM–Fe(II) complex at 5′-GT-3′ scission site. The released G-tetrads DNA fragment further binds hemin to form a G-quadruplex-hemin DNAzyme, which can effectively catalyze the oxidation of ABTS by H_2O_2 to produce a green color. The determination of BLM is thus realized by measuring the absorbance at a wavelength of 420 nm using a UV-Vis spectrophotometer. The colorimetric sensing strategy shows high sensitivity and good selectivity for BLM detection, and it exhibits good assay performance in human serum samples.

Experimental section

Materials and reagents

Bleomycin (BLM) was purchased from Melone Pharmaceutical Co., Ltd. (Dalian, China). Streptomycin, kanamycin, oxytetracycline, chloramphenicol, ampicillin, tobramycin, cisplatin and 5-fluorouracil were obtained from Aladdin Industrial Corporation (Shanghai, China). Glucose, arginine, urea, 2,2′-azinobis(3-ethylbenzthiazoline-6-sulfonic acid) (ABTS), hemin, and doxorubicin were purchased from Sangon Biotech Co., Ltd. (Shanghai, China). H_2O_2, $FeCl_2$ and other analytical reagents were obtained from Sinopharm Chemical Reagent Co., Ltd (Shanghai, China) and used as received without further purification. A 10 mM sodium phosphate buffer containing 100 mM NaCl, and 5 mM KCl (PBS, pH 7.5) was used in the experiments. Ultrapure water with a resistivity of 18.2 MΩ cm obtained from a Millipore Milli-Q water purification system was used throughout the experiments. Oligonucleotide (5′-TGGGTAGGGCGGGTTGGGATTAATTTGTTTTTAATCCC-3′, G4HP) was synthesized and purified by Sangon Biotech Co., Ltd. (Shanghai, China).

Colorimetric detection of BLM

The oligomucleotide G4HP was used as received and diluted in PBS buffer. The BLM–Fe(II) complex was prepared by mixing BLM with $FeCl_2$ in 1 : 1 molar ratio. Subsequently, 40 μL of G4HP (1.5 μM) and 50 μL of hemin (3 μM) were added to the as-prepared BLM–Fe(II) complex, and then incubated at 37 °C for 30 min for the oxidative cleavage of G4HP and the formation of G-quadruplex-hemin DNAzyme. Colorimetric measurements were performed by mixing the above solution with 10 μL of ABTS (4.5 μM), and 10 μL of H_2O_2 (30 mM). The obtained mixture was incubated at room temperature for about 10 min. Finally, the UV-Vis absorbance spectra of the resulting solution were recorded using a UV-6100 spectrophotometer (Metash, Shanghai), and the absorbance at 420 nm was measured to determine the concentration of BLM.

Real samples analysis

For the determination of BLM in real complex samples, recovery experiment by using the standard addition method was carried out by adding four different concentrations of BLM (50 nM, 300 nM, 500 nM, and 800 nM) into the diluted serum sample, followed by colorimetric measurements. Human serum samples of healthy persons were kindly supplied by Sun Yat-Sen University Cancer Center (Guangzhou, China) and diluted 200 times with PBS buffer (10 mM, pH 7.5).

Results and discussion

Principle of the colorimetric sensing strategy

A label-free and sensitive colorimetric sensing strategy for BLM detection was developed on the basis of BLM-mediated activation of G-quadruplex DNAzyme *via* DNA strand scission, which is illustrated in Scheme 1. The G-quadruplex based hairpin probe (G4HP) contains two function domains: a 5′-GT-3′ scission site of BLM at the loop region; the four G-tetrads with the first one of which is locked in the stem of the G4HP, thereby inhibiting the formation of G-quadruplex-hemin DNAzyme. In the presence of BLM, the G4HP undergoes an irreversible cleavage event at the 5′-GT-3′ site *via* the oxidative effect of BLM with Fe(II) as a cofactor, releasing the G-tetrads DNA fragment, which further binds hemin to form a G-quadruplex-hemin DNAzyme. The resultant G-quadruplex DNAzyme can effectively catalyze the oxidation of ABTS by H_2O_2 to induce a distinct color change from colorless to green. Therefore, the colorimetric detection of BLM can be achieved by observing the color transition with the naked eye or measuring the absorbance at a wavelength of 420 nm using a UV-Vis spectrophotometer.

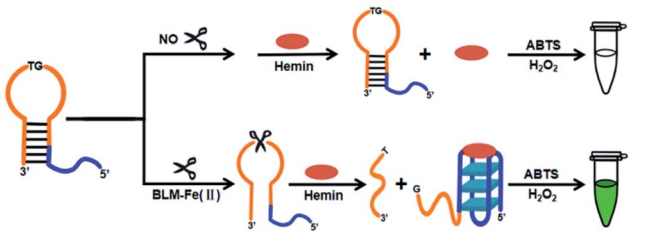

Scheme 1 Schematic illustration of the G-quadruplex based hairpin probe (G4HP) sensing system for BLM detection.

Feasibility of the colorimetric sensing strategy

To demonstrate the feasibility of the G-quadruplex based hairpin probe (G4HP) sensing system for the colorimetric detection of BLM, the color changes and UV-Vis spectra of the H_2O_2–ABTS mixture under different conditions were investigated. As shown in Fig. 1, the peak absorbance at 420 nm was not obvious when adding BLM to H_2O_2-ABTS (curve a) or Fe(II)–H_2O_2–ABTS (curve b) mixtures, and the solution was colorless, which indicated that the BLM enhanced Fe(II)–H_2O_2–ABTS reaction displayed poor efficiency when the concentration of Fe^{2+} was below 5 μM.[22] In addition, adding G4HP to H_2O_2-ABTS (vial 3, inset) or Fe(II)–H_2O_2–ABTS (vial 4, inset) mixtures did not induce a color change and a remarkable increase in the absorbance at 420 nm, indicating that the four G-tetrads was effectively locked in the stem of the G4HP and thus no G-quadruplex-hemin DNAzyme was generated. However, the peak absorbance at 420 nm sharply increased upon incubation with BLM–Fe(II) complex (curve f), and the color of the solution changed from colorless to green (vial 6, inset), indicating the occurrence of BLM–Fe(II) induced DNA strand scission at the loop region of G4HP to release the G-tetrads DNA fragment which can self-assemble into a G-quadruplex-hemin DNAzyme with notable peroxidase-like catalytic activity. Therefore, the G4HP based sensing system can be applied for label-free colorimetric detection of BLM.

Optimization of assay conditions

To achieve the best assay performance for BLM detection, some important experimental conditions were systematically investigated. First, the effect of ABTS concentration on the colorimetric signal was investigated. As shown in Fig. 2A, the absorbance change ($\Delta A = A - A_0$) was enhanced significantly with the increase of ABTS concentration from 100 to 300 μM, followed by the decrease beyond 300 μM (where A_0 and A were the peak absorbance at 420 nm of the sensing system with or without BLM, respectively). Hence, 300 μM was chosen as the optimum ABTS concentration for the subsequent experiments. Meanwhile, the effect of hemin concentration on the sensing performance was investigated. It could be observed that the value of ΔA increased as the hemin concentration increased from 0.1 to 1.0 μM and tended to be constant when the concentration was higher than 1.0 μM (Fig. 2B). Thus, the hemin concentration of 1.0 μM was adopted in the following experiments. In addition, the effect of G4HP concentration and the reaction time on the peak absorbance of the sensing system were also investigated. As shown in Fig. 2C, with the concentration of G4HP increased from 0.2 to 0.4 μM, the value of ΔA significantly increased and leveled off when the G4HP concentration was above 0.4 μM. As shown in Fig. 2D, the ΔA increased rapidly with the reaction time until 30 min, and then tended to be constant. As a result, the G4HP concentration of 0.4 μM and reaction time of 30 min were selected in the detection of BLM.

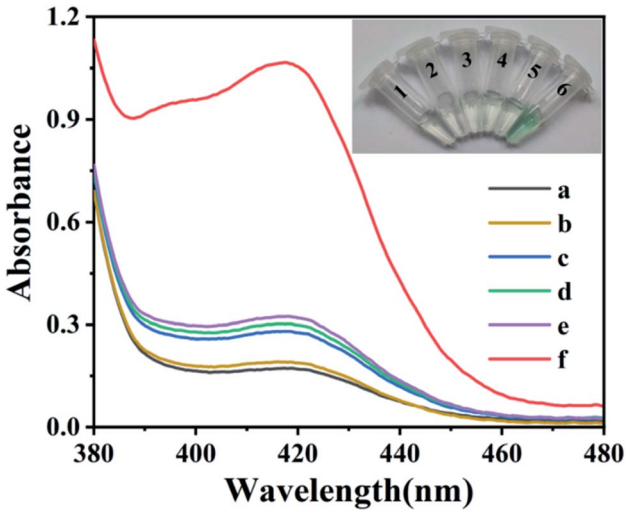

Fig. 1 UV-Vis spectra of the H_2O_2–ABTS mixture toward various circumstances. Inset: photographs of color changes. (1) H_2O_2 + ABTS + BLM; (2) H_2O_2 + ABTS + BLM + Fe^{2+}; (3) H_2O_2 + ABTS + G4HP; (4) H_2O_2 + ABTS + G4HP + Fe^{2+}; (5) H_2O_2 + ABTS + G4HP + BLM; (6) H_2O_2 + ABTS + G4HP + Fe^{2+} + BLM. Concentrations of H_2O_2, ABTS, G4HP, Fe^{2+} and BLM were 2 mM, 300 μM, 0.4 μM, 1 μM and 1 μM, respectively.

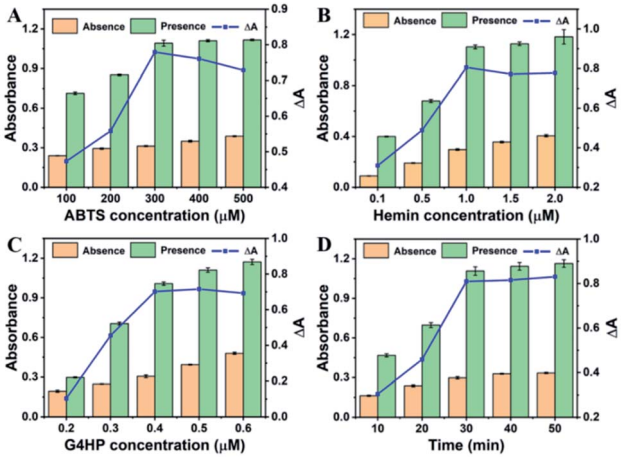

Fig. 2 Optimization of the experimental conditions for BLM detection: the concentrations of ABTS (A), hemin (B), G4HP (C), and reaction time (D). $\Delta A = A - A_0$, where A_0 and A were the peak absorbance at 420 nm of the sensing system with or without BLM, respectively. Error bars represented the standard deviation of three measurements.

Analytical performance for BLM detection

Under optimal conditions, the analytical performance of the G4HP based sensing system was investigated. Fig. 3A displayed the UV-Vis spectra corresponding to different concentrations of BLM. The absorbance at 420 nm of the sensing system increased significantly with the increase of BLM concentration ranging from 0 to 10 μM, and the color of solution gradually changed from colorless to green (Fig. 3B). A linear calibration curve was obtained by plotting the absorption intensity at 420 nm against the BLM concentration over the range from 10 nM to 1 μM (Fig. 3C). The regression equation is $A = 0.28014 + 0.82307C$ ($R^2 = 0.9967$), where A and C represent the absorption intensity at 420 nm and the BLM concentration, respectively. The detection limit was estimated to be as low as 5 nM

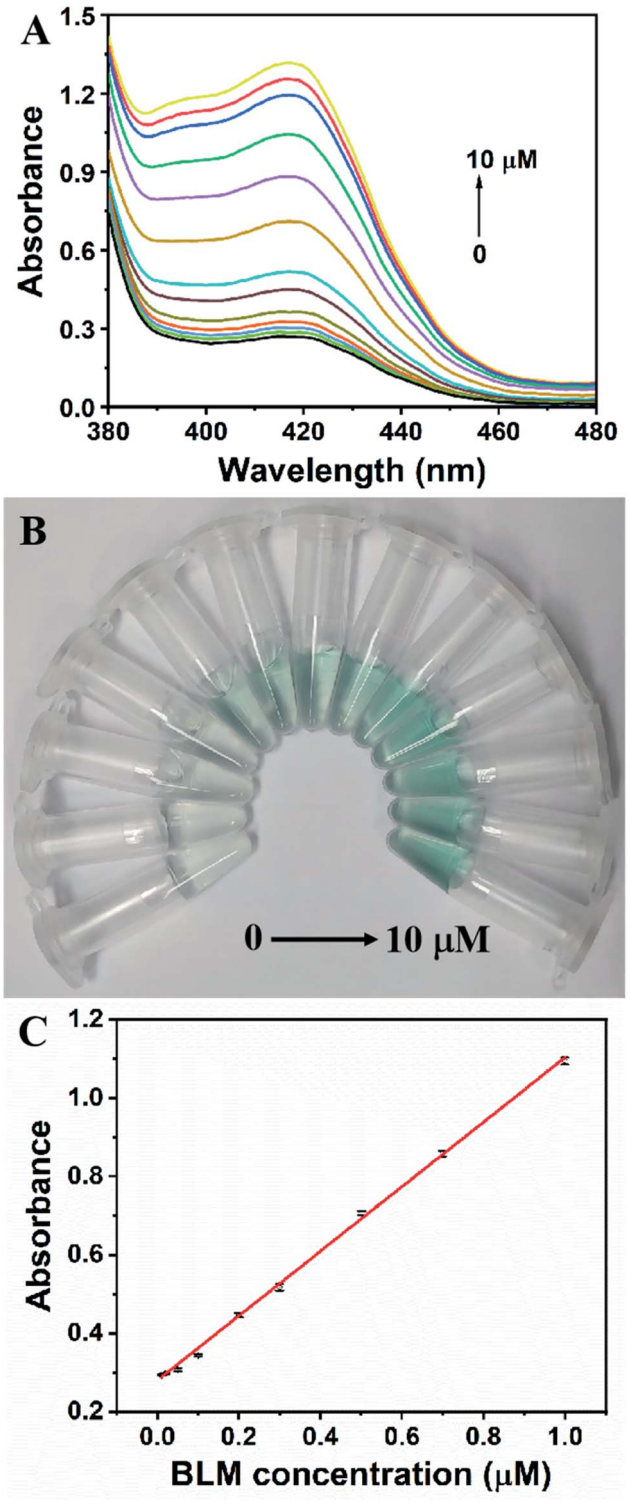

Fig. 3 UV-Vis absorption spectra (A) and color changes (B) of the G4HP based sensing system in the presence of different concentrations of BLM (0, 10, 20, 50, 100, 200, 300, 500, 700, 1000, 1500, 2000, 5000 and 10 000 nM). (C) Linear relationship of the absorption intensity at 420 nm *versus* the BLM concentration ranging from 10 nM to 1 μM. Error bars indicated the standard deviations of three measurements.

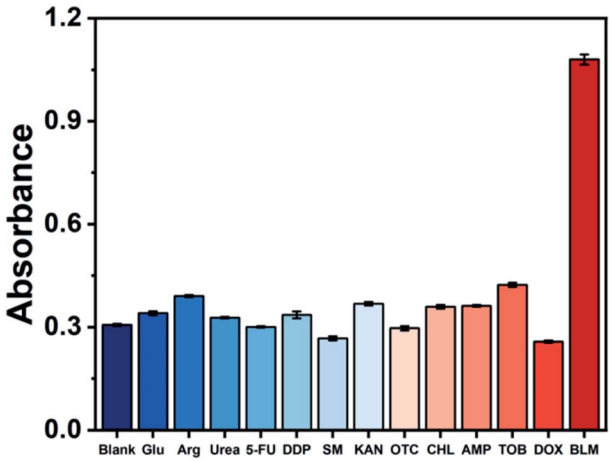

Fig. 4 Selectivity of the G4HP based sensing system for BLM detection against other potential interferences. The concentrations of all interfering substances were 10 μM, the concentration of BLM was 1 μM. Error bars were estimated from three replicate measurements.

with a signal-to-noise ratio of 3. Meanwhile, the assay volume of 0.15 mL and the assay time of 40 min needed to complete the detection of BLM, which are comparable to those of the existing sensing strategies for BLM detection (Table S1†). To evaluate the selectivity of the colorimetric sensing strategy, various other potential interferences including glucose (Glu), arginine (Arg), urea, 5-fluorouracil (5-FU), cisplatin (DDP), streptomycin (SM), kanamycin (KAN), oxytetracycline (OTC), chloramphenicol (CHL), ampicillin (AMP), tobramycin (TOB) and doxorubicin (DOX) were added into the sensing system, respectively. As shown in Fig. 4, only upon addition of BLM, a remarkable change in the absorbance at 420 nm could be induced due to the specific DNA scission, whereas the absorbance of one of the twelve interfering substances were fairly low and exhibited no conspicuous difference compared with that of blank sample, indicating that the G4HP based sensing system exhibited high specificity for discriminating BLM from other interfering substances.

Human serum samples analysis

In order to evaluate the practical applicability of the colorimetric sensing strategy in complex biological samples, recovery experiments by applying the standard addition method in human serum samples were carried out. Four different concentrations of BLM were separately spiked in the diluted serum sample and detected by the proposed method. As shown in Table 1, the recoveries of the four samples were in the range

Table 1 Detection of BLM in human serum samples

Sample	Added (nM)	Found (nM)	Recovery (%)	RSD ($n = 3$, %)
1	50	47.6	95.2	2.76
2	300	290.0	96.6	1.66
3	500	506.8	101.4	3.11
4	800	830.0	103.8	1.34

of 95.2–103.8% with the relative standard deviations (RSDs) less than 3.11%, indicating that the developed method has potential application for BLM assay in complex real samples.

Conclusions

In summary, we have developed a label-free and sensitive G-quadruplex based hairpin probe (G4HP) sensing system for colorimetric detection of BLM based on BLM-mediated activation of G-quadruplex DNAzyme *via* DNA strand scission. Under the oxidative effect of BLM with Fe(II) as a cofactor, the G4HP undergoes an irreversible cleavage event at the loop region that contains 5′-GT-3′ recognition site for BLM. The released G-tetrads DNA fragment further binds hemin to form a G-quadruplex-hemin DNAzyme, which can effectively catalyze the H_2O_2-meiated oxidation of ABTS to induce a distinct color change from colorless to green. Therefore, the detection of BLM can be achieved by observing the color transition or measuring the absorbance at a wavelength of 420 nm. Due to the high efficiency of BLM-activated G-quadruplex DNAzyme catalysis, the colorimetric sensing strategy exhibited a high sensitivity with a detection limit of 5 nM in a linear range of 10–1000 nM. Moreover, the application of the proposed method for BLM detection in human serum samples was also implemented with satisfactory results due to its excellent selectivity. Considering these merits, the colorimetric sensing strategy may provide with great potential for BLM determination in clinical samples.

Author contributions

Xiaofei Liao: data curation, formal analysis, investigation, methodology. Mengyan Li: investigation, validation, visualization. Li Zou: conceptualization, funding acquisition, project administration, supervision, writing – original draft, writing – review & editing.

Conflicts of interest

There are no conflicts to declare.

Acknowledgements

This work was supported by the National Natural Science Foundation of China (No. 81903570) and the Natural Science Foundation of Guangdong Province (No. 2021A1515011519).

References

1 H. Umezawa, K. Maeda, T. Takeuchi and Y. Okami, *J. Antibiot.*, 1966, **19**, 200–209.
2 U. Galm, M. H. Hager, S. G. Van Lanen, J. Ju, J. S. Thorson and B. Shen, *Chem. Rev.*, 2005, **105**, 739–758.
3 T. C. Bozeman, R. Nanjunda, C. Tang, Y. Liu, Z. J. Segerman, P. A. Zaleski, W. D. Wilson and S. M. Hecht, *J. Am. Chem. Soc.*, 2012, **134**, 17842–17845.
4 G. Tisman, V. Herbert, L. T. Go and L. Brenner, *Blood*, 1973, **41**, 721–726.
5 J. Stubbe and J. W. Kozarich, *Chem. Rev.*, 1987, **87**, 1107–1136.
6 C. A. Claussen and E. C. Long, *Chem. Rev.*, 1999, **99**, 2797–2816.
7 R. A. Giroux and S. M. Hecht, *J. Am. Chem. Soc.*, 2010, **132**, 16987–16996.
8 J. Hay, S. Shahzeidi and G. Laurent, *Arch. Toxicol.*, 1991, **65**, 81–94.
9 E. Azambuja, J. F. Fleck, R. G. Batista and S. S. Menna Barreto, *Pulm. Pharmacol. Ther.*, 2005, **18**, 363–366.
10 R. P. Klett and J. P. Chovan, *J. Chromatogr., Biomed. Appl.*, 1985, **337**, 182–186.
11 J. D. Teale, J. M. Clough and V. Marks, *Br. J. Cancer*, 1977, **35**, 822–827.
12 K. Fujiwara, M. Isobe, H. Saikusa, H. Nakamura, T. Kitagawa and S. Takahashi, *Cancer Treat. Rep.*, 1983, **67**, 363–369.
13 T. Onuma, J. F. Holland, H. Masuda, J. A. Waligunda and G. A. Goldberg, *Cancer*, 1974, **33**, 1230–1238.
14 F. Li, Y. Feng, C. Zhao and B. Tang, *Biosens. Bioelectron.*, 2011, **26**, 4628–4631.
15 X. Liu, W. Na, Q. Liu and X. Su, *Anal. Chim. Acta*, 2018, **1028**, 45–49.
16 S. Zhu, L. Liu, J. Sun, F. Shi and X. Zhao, *Spectrochim. Acta, Part A*, 2021, **252**, 119521.
17 D. Zhang, J. Hu, X. Yang, Y. Wu, W. Su and C. Zhang, *Nanoscale*, 2018, **10**, 11134–11142.
18 Y. He, Y. Gao, H. Gu, X. Meng, H. Yi, Y. Chen and W. Sun, *Biosens. Bioelectron.*, 2021, **178**, 113034.
19 J. Chang, P. Gai, H. Li and F. Li, *Talanta*, 2018, **190**, 492–497.
20 Y. Song, W. Wei and X. Qu, *Adv. Mater.*, 2011, **23**, 4215–4236.
21 X. Zhang, Y. Zhang, H. Zhao, Y. He, X. Li and Z. Yuan, *Anal. Chim. Acta*, 2013, **778**, 63–69.
22 Y. Qin, L. Zhang, G. Ye and S. Zhao, *Anal. Methods*, 2014, **6**, 7973–7977.
23 G. Xu and M. R. Chance, *Chem. Rev.*, 2007, **107**, 3514–3543.
24 R. A. Giroux and S. M. Hecht, *J. Am. Chem. Soc.*, 2010, **132**, 16987–16996.
25 B. Yin, D. Wu and B. Ye, *Anal. Chem.*, 2010, **82**, 8272–8277.
26 F. Li, Y. Feng, C. Zhao, P. Li and B. Tang, *Chem. Commun.*, 2012, **48**, 127–129.
27 Y. Qin, Y. Ma, X. Jin, L. Zhang, G. Ye and S. Zhao, *Anal. Chim. Acta*, 2015, **866**, 84–89.
28 H. Li, J. Chang, T. Hou and F. Li, *Anal. Chem.*, 2017, **89**, 673–680.
29 S. Cheng, M. Khan, L. Luo, L. Wang, S. Liu, J. Ping, J. Lin and Q. Hu, *Anal. Chim. Acta*, 2021, **1150**, 338247.
30 L. Ma, X. Han, L. Xia, R. Kong and F. Qu, *Analyst*, 2018, **143**, 5474–5480.
31 H. Peng, A. M. Newbigging, Z. Wang, J. Tao, W. Deng, X. C. Le and H. Zhang, *Anal. Chem.*, 2018, **90**, 190–207.
32 R. Freeman, E. Sharon, C. Teller, A. Henning, Y. Tzfati and I. Willner, *ChemBioChem*, 2010, **11**, 2362–2367.
33 Y. Lai, M. Li, X. Liao and L. Zou, *Molecules*, 2021, **26**, 5016.
34 Y. M. Xie, F. N. Niu, A. M. Yu and G. S. Lai, *Anal. Chem.*, 2020, **92**, 593–598.
35 Y. Gao and B. X. Li, *Anal. Chem.*, 2013, **85**, 11494–11500.
36 P. Zhang, X. Y. Wu, R. Yuan and Y. Q. Chai, *Anal. Chem.*, 2015, **87**, 3202–3207.